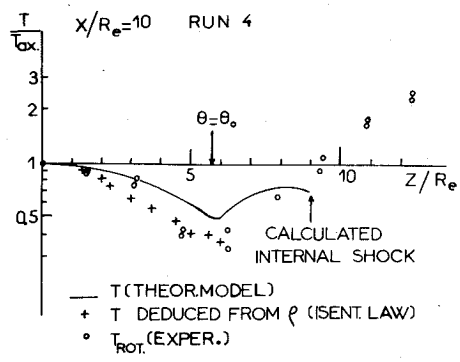

Fig. 3 Transverse profiles; temperature.

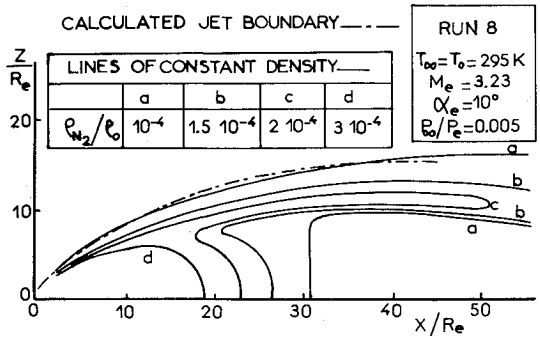

Fig. 4 Jet boundary and lines of constant density.

corresponds to $\theta=\theta_o=29.8°$. This is because of the gradient of static temperature in the exit section of the nozzle, when entering the boundary layer. As the model does not describe the viscous layer, the comparison with the experimental profile must be restricted to the region between the axis and the internal shock. The measured profile exhibits the same overall features as the predicted one. A sudden change in the slope is observed at the predicted value of θ_o, a finding which confirms the validity of the determination of θ_o from Eq. (3), But both profiles really do not coincide. The fact that the measured T_r profile coincides with the T_r profile deduced from the ρ profile, using the isentropic relation, suggests that the discrepancy is mainly because of the inadequacy of the semiempirical $f(\theta)$ at such abscissa, and possibly because of the experimental error.

Jet Boundary

Under our experimental conditions, the gas was so rarefied that the flows could be classified in the transition regime. Diffusion phenomena forbid speaking of a well-defined jet boundary. Draper and Sutton[7] consider that the theoretical boundary obtained from a continuum theory then can be interpreted as the line of equal concentration of the external and the ejected gas, provided that both gases had approximately equal molecular weights. We have plotted in Fig. 4 the lines of equal density deduced from the exploration of the flowfield of run 8, and we developed a very simple calculation for determining the position of the line of equal concentration, based on the following assumption.

Near the boundary, a region exists where the external air diffuses into the ejected nitrogen. We consider this region as a boundary layer with a uniform pressure P_∞, a velocity profile U, and a temperature profile T, related to the U profile by means of the modified Crocco relationship,

$$T=T_\infty+(T_f-T_\infty)\,U/U_L-T_f(U/U_L)^2 \tag{5}$$

where the recovery temperature T_f may be approximated by the local total temperature T_t in the jet at the boundary of the viscous layer. Furthermore, the α profile (concentration of ejected gas) is assumed to coincide with the U profile ($\alpha=U/U_L$). Then, simple calculations lead to

$$\frac{\rho_{N_2}}{\rho_o}=\frac{P_\infty T_o}{P_o T_\infty}\,\frac{\alpha+0.79(1-\alpha)}{1+(T_t/T_\infty-1)\alpha-(T_t/T_\infty)\alpha^2} \tag{6}$$

For run 8, the stagnation temperature T_o is equal to T_∞, so that T_t is approximately equal to T_o all along the boundary. The line of equal concentration $\alpha=½$ coincides with the line of constant density

$$\rho_{N_2}/\rho_o=1.19P_\infty T_o/(P_o T_\infty)=1.16\ 10^{-4} \tag{7}$$

Figure 4 shows that the calculated boundary nearly coincides with the line of equal density $\rho_{N_2}/\rho_o=10^{-4}$. Considering the approximations made in the present calculation, a better agreement was not expected. Nevertheless, it seems that the interpretation by Draper and Sutton for the calculated boundary in the transition regime is confirmed to the present experiment.

References

[1] Lengrand, J. C., "Approximate Calculations of Rocket Plumes with Nozzle Boundary Layers and External Pressure," *Proceedings of the Ninth International Symposium on Rarefied Gas Dynamics,* Vol. 1, Deutsche Forschungs- und Versuchsanstalf für Luft- und Raumfahrt Press, Porz-Wahn, Germany, 1974, B 13.

[2] Albini, F. A., "Approximate Computation of Underexpanded Jet Structure," *AIAA Journal*, Vol. 3, Aug. 1965, pp. 1535-1537.

[3] Simons, G. A., "Effect of Nozzle Boundary Layers on Rocket Exaust Plumes," *AIAA Journal*, Vol. 10, Nov. 1972, pp. 1534-1535.

[4] Boynton, F. P., "Highly Underexpanded Jet Structures. Exact and Approximate Calculations," *AIAA Journal*, Vol. 5, Sept. 1967, pp. 1703-1705.

[5] Lengrand, J. C., "Calculs de Jets Sous-Détendus Issus de Tuyéres Supersoniques," Rapport 75-4, Lab. d'Aérothermique du CNRS, Meudon, France.

[6] Muntz, E. P., "Static Temperature Measurement in a Flowing Gas," *Physics of Fluids*, Vol. 5, Jan. 1962, pp. 80-90.

[7] Draper, J. S. and Sutton, E. A., "A Nomogram for High-Altitude Plume Structures," *Journal of Spacecraft and Rockets*, Vol. 10, Oct. 1973, pp. 682-684.

Hot-Wire and Vorticity Meter Wake Vortex Surveys

A.D. Zalay*
Lockheed Missiles & Space Company, Inc., Huntsville, Ala.

RECENTLTY, as part of a systematic study on wake vortices, surveys have been conducted using both a hot-wire anemometer and a paddle-wheel-type vorticity meter.[1] As anticipated, the hot-wire and vortex meters gave similar results for concentrated trailing vortices. When the vortex wake was "aged" by turbulent injection, however, the vorticity meter significantly underestimated the strength of the vortex field. Comparisons of the vorticity meter and hot-wire wake vortex surveys, summarized briefly in the following Note, indicate that vorticity meters behave in a nonlinear fashion in weak vortex fields.

Measurements have been conducted of the trailing vortex formed 6.5 chord lengths downstream of a 21-in. chord, rec-

Received Nov. 18, 1975; revision received Jan. 30, 1976. Work done under Office of Naval Research sponsorship as an employee of Rochester Applied Science Associates Division of SRL.

Index categories: Aircraft Aerodynamics (including Component Aerodynamics); Aircraft Testing (including Component Wind Tunnel Testing; Jets, Wakes, and Viscid-Inviscid Flow Interactions.

*Senior Research Engineer. Member AIAA.

tangular, $AR=5.6$ airfoil with an NACA 0012 profile, operating at $U_\infty = 150$ fps, $Re = 1.6\times10^6$, $C_L = 0.57$, and $C_D = 0.045$. The tangential and axial velocity profile of the trailing vortex is shown in Fig. 1 as measured by a three-component hot-wire system traversed rapidly (~20 ips) across the vortex, with and without axial injection. Note that the injection of a turbulent jet from a 0.5-in.-diam. sonic nozzle, $\dot{m} = 0.12$ lb/sec, into the center of the vortex spreads the viscous core but leaves the outer potential flow essentially unchanged. This trend agrees with previous measurements conducted by other investigators.[2,3] Additional information on the mean and turbulent velocity characteristics of the vortex and the hot-wire instrumentation systems and calibration is available in Ref. 1.

The wake vortex surveys presented in Fig. 1 have been repeated, using a vorticity meter. As described in Ref. 4, the vorticity meter consists of a paddle-wheel sensor mounted on a rotating shaft and fitted with a jeweled bearing. Calibration of the vorticity meter is accomplished by attaching a "calibration collar," fixed-vane-type swirl generator, to the device. The efficiency of the vorticity meter is established as a function of different axial velocities according to the relation, $\eta = 1/[1+(k/V_x)]$, where η is the ratio of the rotational velocity of the vanes to that of the fluid, V_x is the axial velocity at the probe location, and k is a calibration constant taken to be equal to 27.8. For the present test sequence, the efficiency factor of the vorticity meter ranged from $\eta = 0.85$ to 0.90 and included a minor correction resulting from the axial component of the turbulent jet at the probe location.

The survey of the trailing vortex by the vorticity meter is presented in Fig. 2. Note the relatively low level of scatter and apparent axial symmetry of the trailing vortex which has been noted also in the hot-wire measurements. To compare the hot-wire and vorticity meter surveys shown in Figs. 1 and 2, the measurements have been integrated to yield the circulation of the trailing vortex presented in Fig. 3. From the results shown in Fig. 3, it is seen that the circulation measured by the hot-wire and the vorticity meter are in close agreement, for the concentrated trailing vortex. When the vortex core is spread by the turbulent jet as characteristic of an "aged" vortex, however, the vorticity meter indicates a significantly lower circulation strength than the hotwire. Indeed, according to the vorticity meter, turbulent injection reduces the total vortex strength to one-third the nominal value, an interesting development in the light of Kelvin's conservation of vorticity theorem.

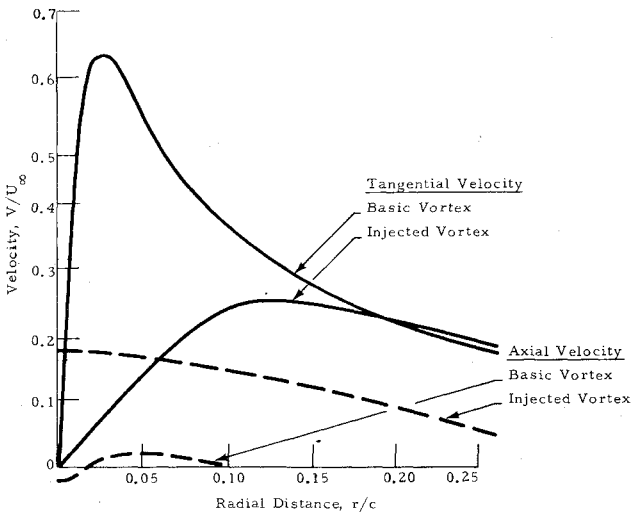

Fig. 1 Tangential and axial velocity profile of trailing vortex measured by a three-component hot-wire anemometer system.

Comparing the hot-wire and vorticity meter surveys for the "aged" vortex, it can be seen that the vorticity meter shows a constant circulation strength and zero vorticity for $r/c > 0.14$. The hot-wire shows, however, that there is a vorticity at extended radial distances, i.e., $r/c > 0.14$; and, in fact, a slight circulation overshoot exists in comparison to the unmodified concentrated vortex. It would appear that the vorticity meter is less sensitive than the hot-wire in weak vorticity fields. There is no calibration available to account for this nonlinearity.

Since wake vortex surveys have been conducted by several investigatiors under approximately the same test conditions using hot wire, laser velocimeter, and yawhead pressure probe measurements, it is useful to compare these and the present results. A summary of wind-tunnel wake vortex measurements is shown in Table 1, where the circulation parameters Γ_c/ν and r_c/c are the dimensionless core circulation and core radius of the trailing vortex, respectively. From the measurements given in Table 1, a substantial increase in the radius of the viscous vortex can be noted when a momentum deficit or excess is introduced into the core region. In addition to increasing the core radius, the wingtip mounted drag or thrust producing devices also increase the core circulation of

Table 1 Comparison of trailing vortex measurements

Investigator	Survey	x/c	C_L	AR	$Re\times10^{-5}$	$\Gamma_c/\nu\times10^{-4}$	r_c/c	Comment
Corsiglia et al.[7]	Rotating hot wire	53.0	0.65	5.3	9.0	9.6	0.05	Clean wing
		53.0	0.65	5.3	9.0	13.9	0.21	Wing with tip spoiler
Orloff and Grant[8]	Laser doppler velocimeter	7.0	0.80	5.3	7.3	13.6	0.09	Clean wing
		7.0	0.80	5.3	7.3	18.3	0.09	Wing with tip spoiler
Marchman and Uzel[9]	Pressure probe	10.0	0.67	12.0	2.8	7.9	0.09	Clean wing
		10.0	0.67	12.0	2.8	7.9	0.38	Wing with tip spoiler
Present Tests[1]	Hot-wire traverse	6.5	0.57	5.6	16.4	19.6	0.03	Clean wing
	Vorticity meter	6.5	0.57	5.6	16.4	26.1	0.05	Clean wing
	Hot-wire traverse	6.5	0.57	5.6	16.4	33.5	0.12	Wing with vortex injection
	Vorticity meter	6.5	0.57	5.6	16.4	13.9	0.08	Wing with vortex injection

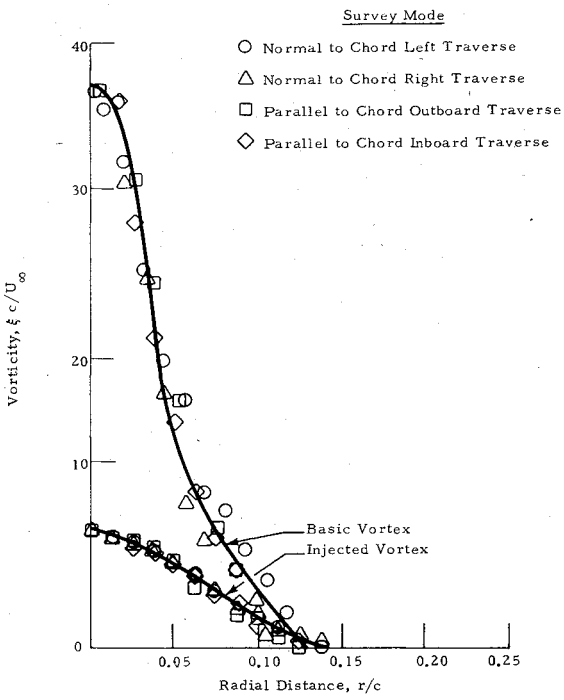

Fig. 2 Vorticity of trailing vortex measured by vorticity meter.

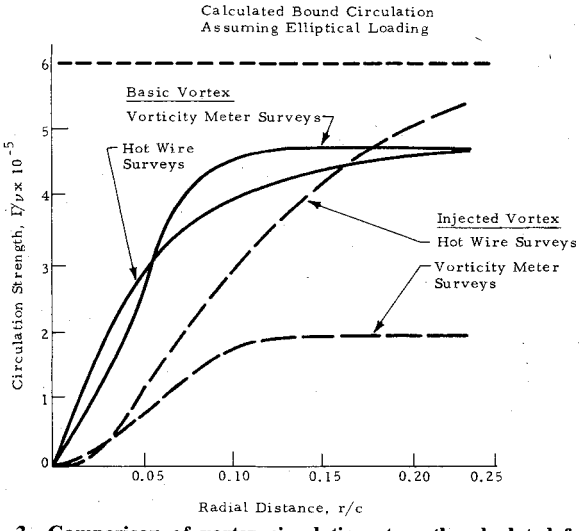

Fig. 3 Comparison of vortex circulation strength calculated from vorticity meter and hot-wire measurements.

the vortex as shown by the hotwire, laser velocimeter, and pressure probe measurements. On the other hand, the vorticity meter surveys indicate the opposite trend, a decrease in the core circulation with vortex injection. Thus, the vorticity meter measurements are not consistent with the hot-wire surveys or with the trends obtained by other measurement techniques.

Although vorticity meters have been used often to measure vortex flows, no study has been done to compare the vorticity meter with other flow measuring devices. Comparisons of the vorticity meter and hot-wire system discussed in this note indicate that the vorticity meter behaves in a nonlinear fashion for weak vortex flows. This may explain the low vortex circulations cited in Refs. 4-6 and avert future misunderstandings.

References

[1]Zalay, A.D., White, R.P., and Balcerak, J.C., "Investigation of Viscous Line Vortices With and Without the Injection of Core Turbulence," Rept. 74-01, Feb. 1974, Rochester Applied Science Associates, Rochester, N.Y.

[2]Poppleton, E.D., "A Preliminary Experimental Investigation of the Structure of a Turbulent Trailing Vortex," TN 71-1, May 1971, McGill University, Montreal, Canada.

[3]Kantha, H.L., Lewellen, W.S., and Durgin, F.H., "Qualitative Responses of a Vortex Core to Tip Blowing and Intersecting Airfoils," ASRL-TR 153-4, Aug. 1971, Massachusetts Institute of Technology, Cambridge, Mass.

[4]McCormick, B.W., Tangler, J.L., and Sherrieb, H.E., "Structure of Trailing Vortices," *Journal of Aircraft*, Vol. 5, March 1968, p. 260.

[5]White, R.P. and Balcerak, J.C., "Investigation of the Dissipation of the Tip Vortex of a Rotor Blade by Mass Injection," TR 72-43, 1972, USAAMRDL, Ft. Eustis, Va., 1972.

[6]Sheath, D.D., "Vortex Airfoil Interaction Tests," *Proceedings of the AIAA 2nd Atmospheric Flight Mechanics Conference*, Sept. 1972, Palo Alto, Calif.

[7]Corsiglia, V.R., Schwind, P.G., and Chigier, N.A., "Rapid Scanning, Three-Dimensional, Hot-Wire Anemometer Surveys for Wing Tip Vortices in the Ames 40-by 80-Foot Wind Tunnel," AIAA Paper 73-629, Palm Springs, Calif., 1973.

[8]Orloff, K.L. and Grant, G.R., "The Application of A Scanning Laser Doppler Velocimeter to Trailing Vortex Definition and Alleviation," AIAA Paper 73-680, Palm Springs, Calif., 1973.

[9]Marchman, J.F., III and Uzel, J.N., "Effect of Several Wing Tip Modifications on a Trailing Vortex," *Journal of Aircraft*, Vol. 9, Sept. 1972, pp. 684-686.

Prediction of Turbulent Boundary Layers at Low Reynolds Numbers

Richard H. Pletcher*
Iowa State University, Ames, Iowa

Introduction

FINITE-DIFFERENCE calculation methods, using eddy-viscosity or mixing length models, have become reasonably well established as efficient and reliable tools for predicting most features ot two-dimensional turbulent wall boundary layers under a fairly wide range of conditions. However, some uncertainty apparently still exists regarding the nature of turbulent flow at low Reynolds numbers, and the form of the turbulence model required to accurately predict this flow using a finite-difference calculation procedure.

Although numerous turbulent models which have been proposed differ in detail, many share the use of damped mixing length evaluation for the turbulent viscosity in the inner region according to the form

$$\mu_{T(\text{inner})} = \rho \ell^2 |\partial u/\partial y| \tag{1}$$

with ℓ being specified for at least part of the inner region as

$$\ell_{(\text{inner})} = \kappa D y \tag{2}$$

where κ is the von Karman constant and D is a damping function which accounts for the effects of the kinematic viscosity on the turbulence near the wall. To a large extent in the outer region, the majority of the simple models employ either a

Received December 18, 1975; revision received February 17, 1976. This work has been supported by the Engineering Research Institute, Iowa State University, through funds provided by the National Science Foundation under Grants GK-18810 and ENG-74-22193.

Index category: Boundary Layers and Convective Heat Transfer—Turbulent.

*Associate Professor, Department of Mechanical Engineering and Engineering Research Institute. Member AIAA.